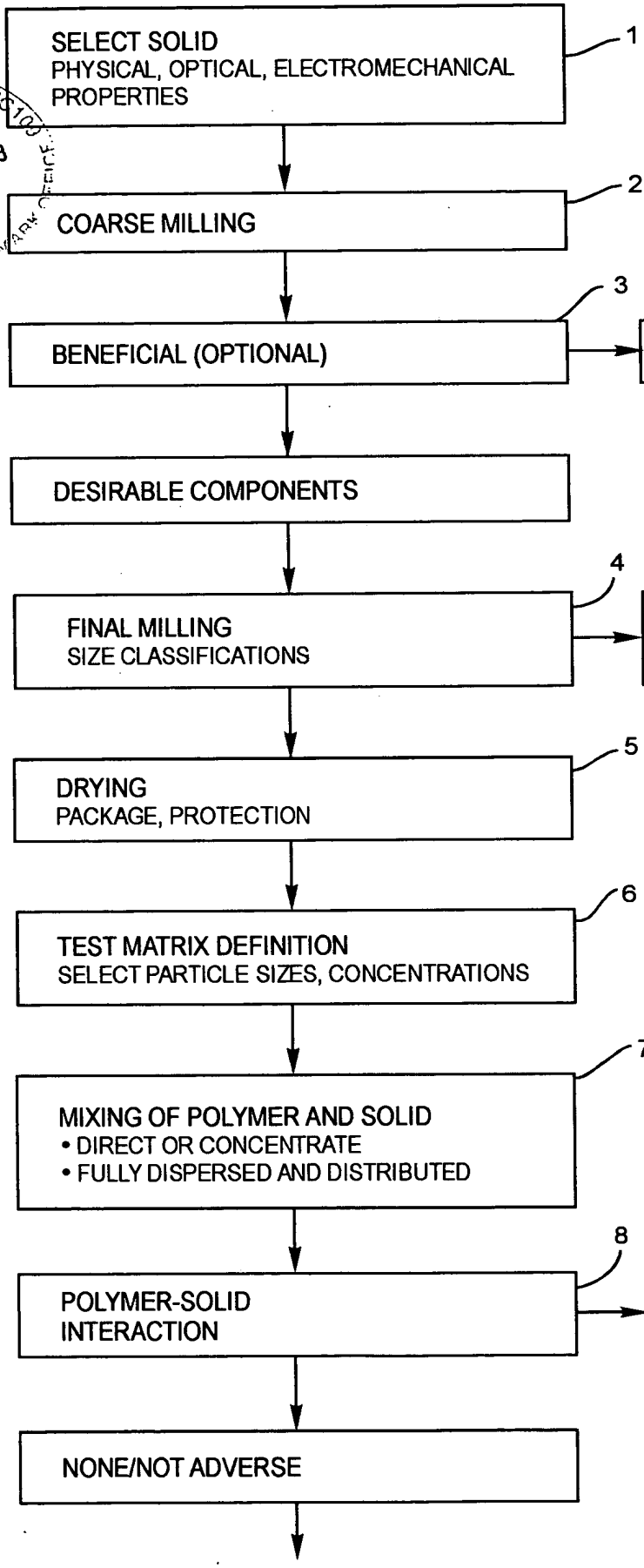

Fig. 1

Fig. 1A

Fig. 1B

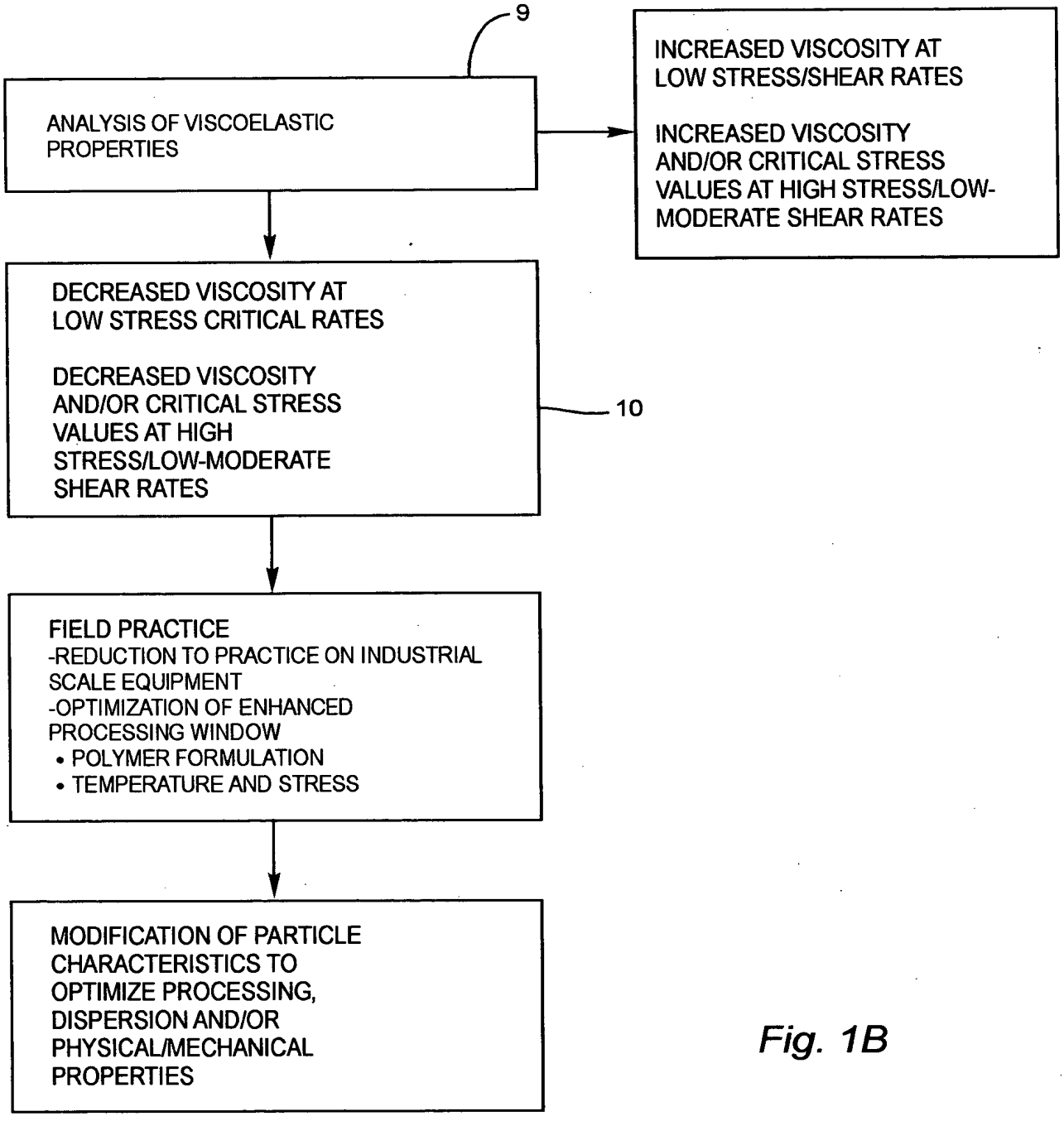

Fig. 1B

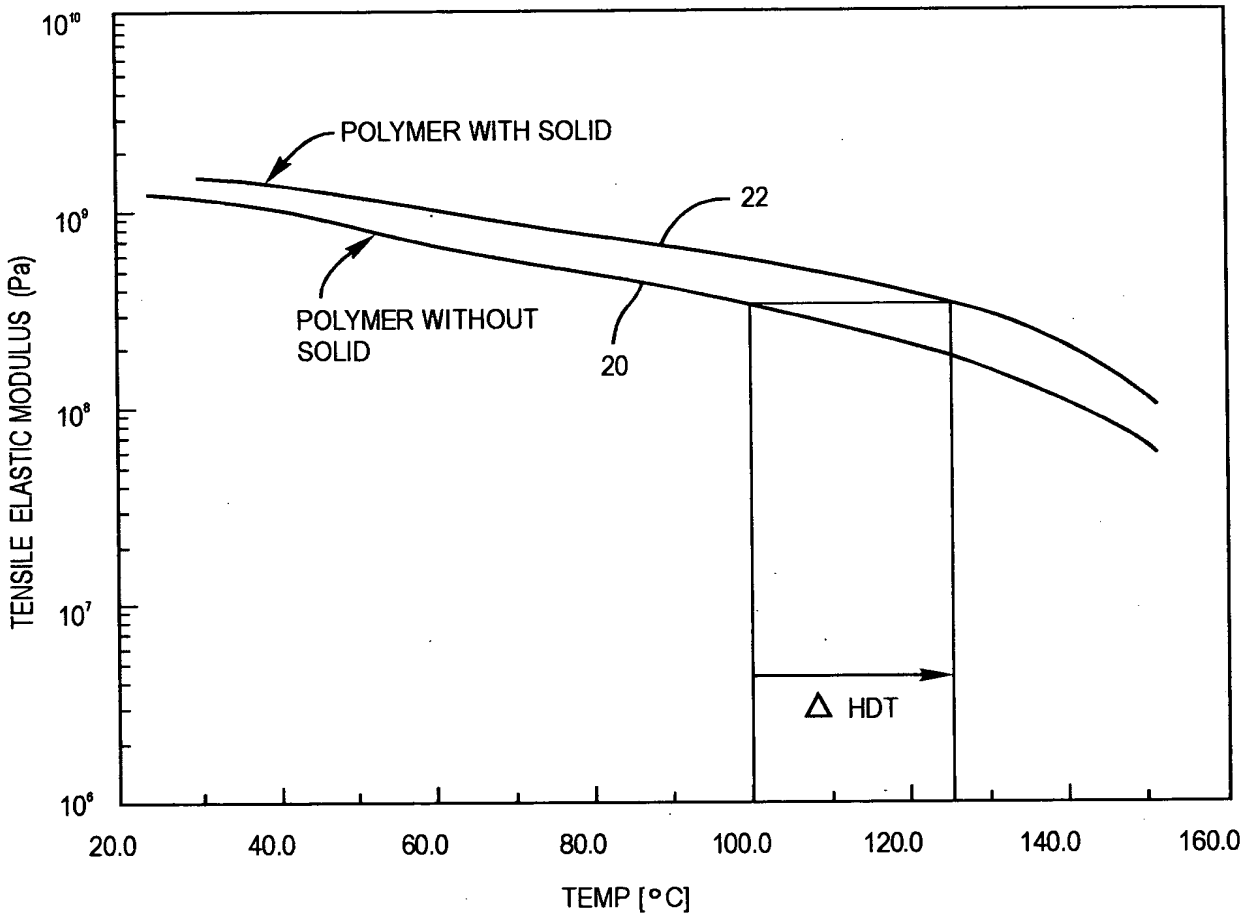

TENSILE ELASTIC MODULUS OF POLYMER AS FUNCTION OF TEMPERATURE

Fig. 2

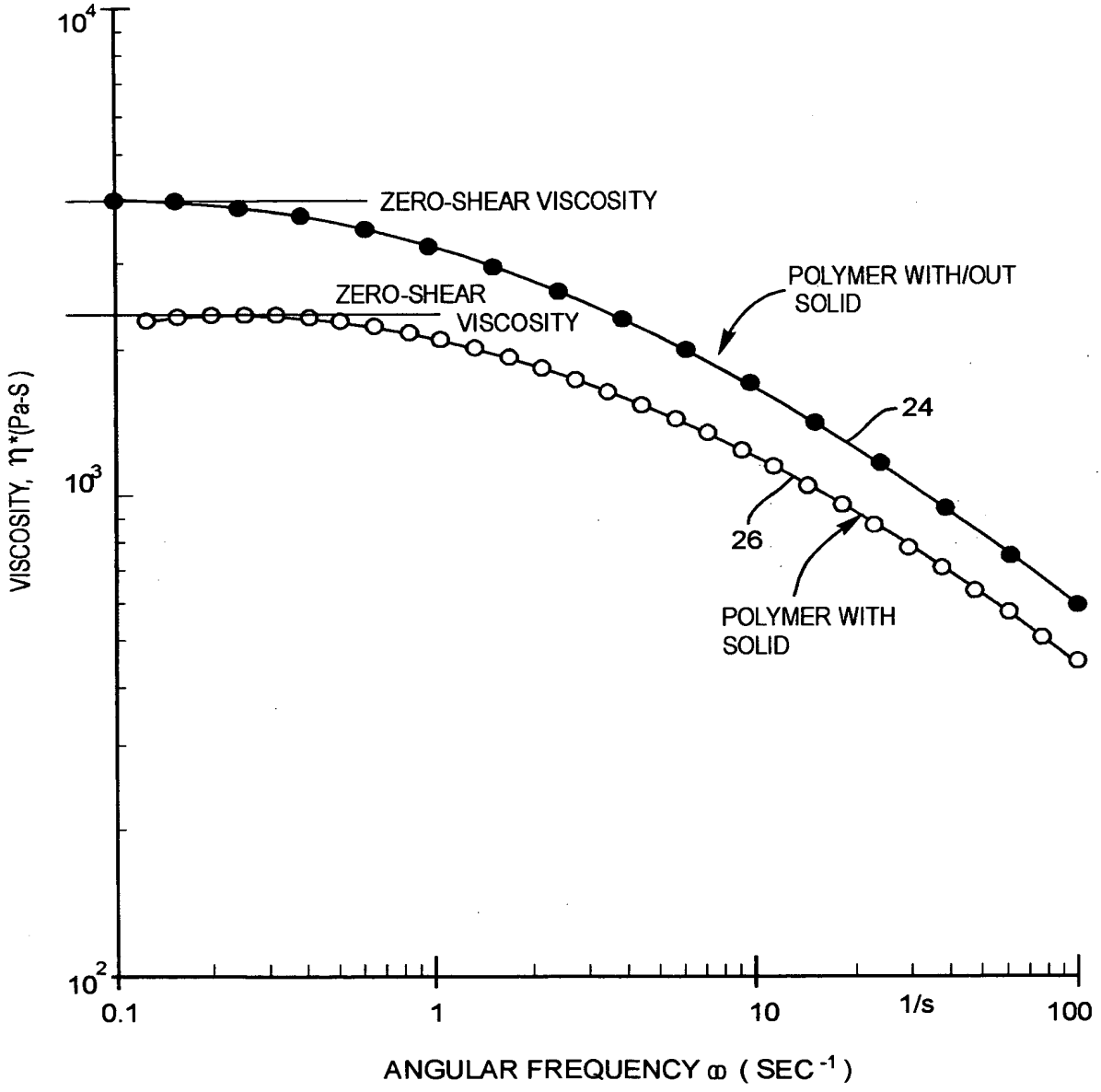

DETERMINATION OF ZERO-SHEAR VISCOSITY FROM VISCOSITY-FREQUENCY PLOT

Fig. 3

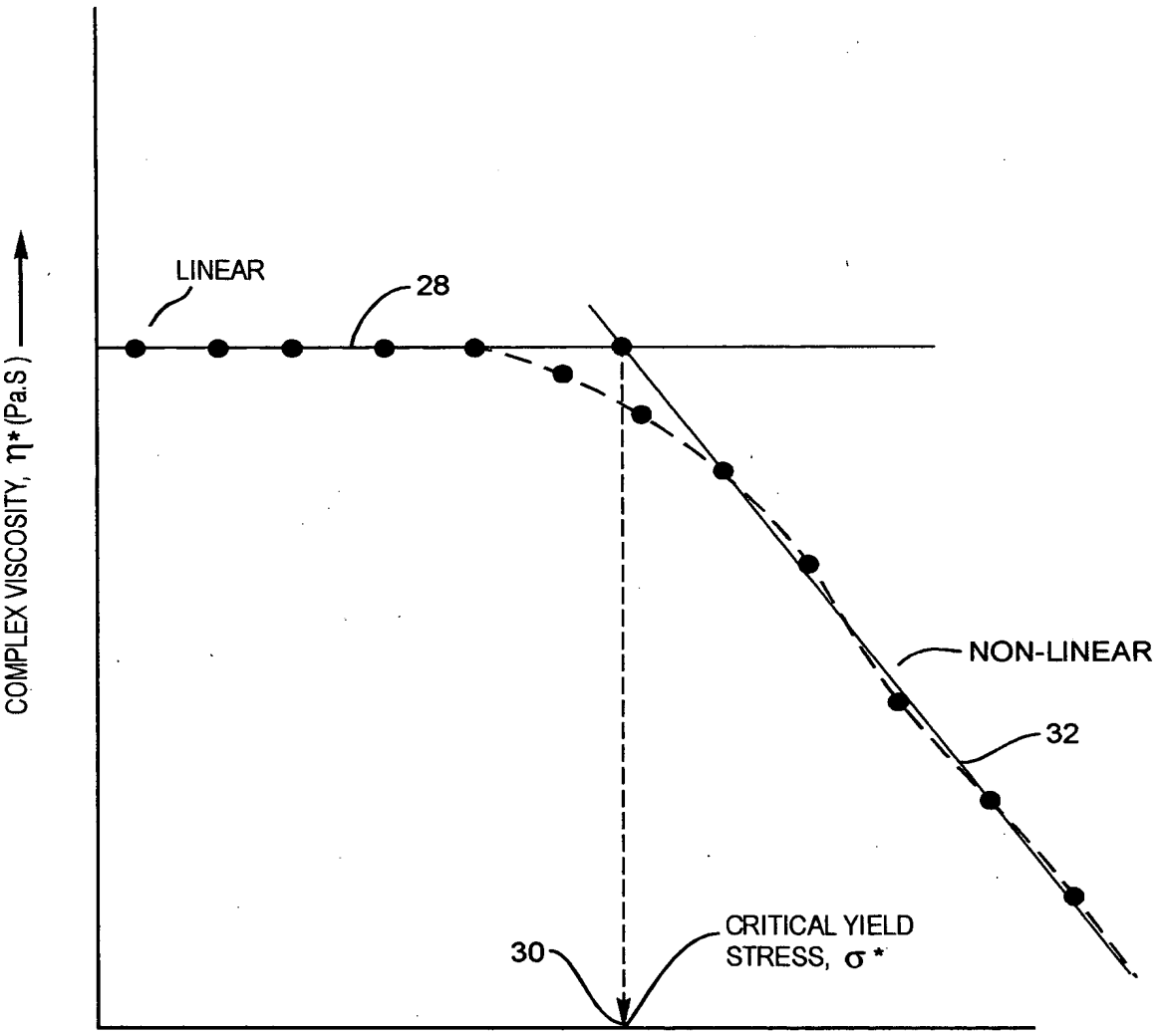

DETERMINATION OF CRITICAL STRESS VALUE FROM VISCOSITY-STRESS CURVES.

Fig. 4

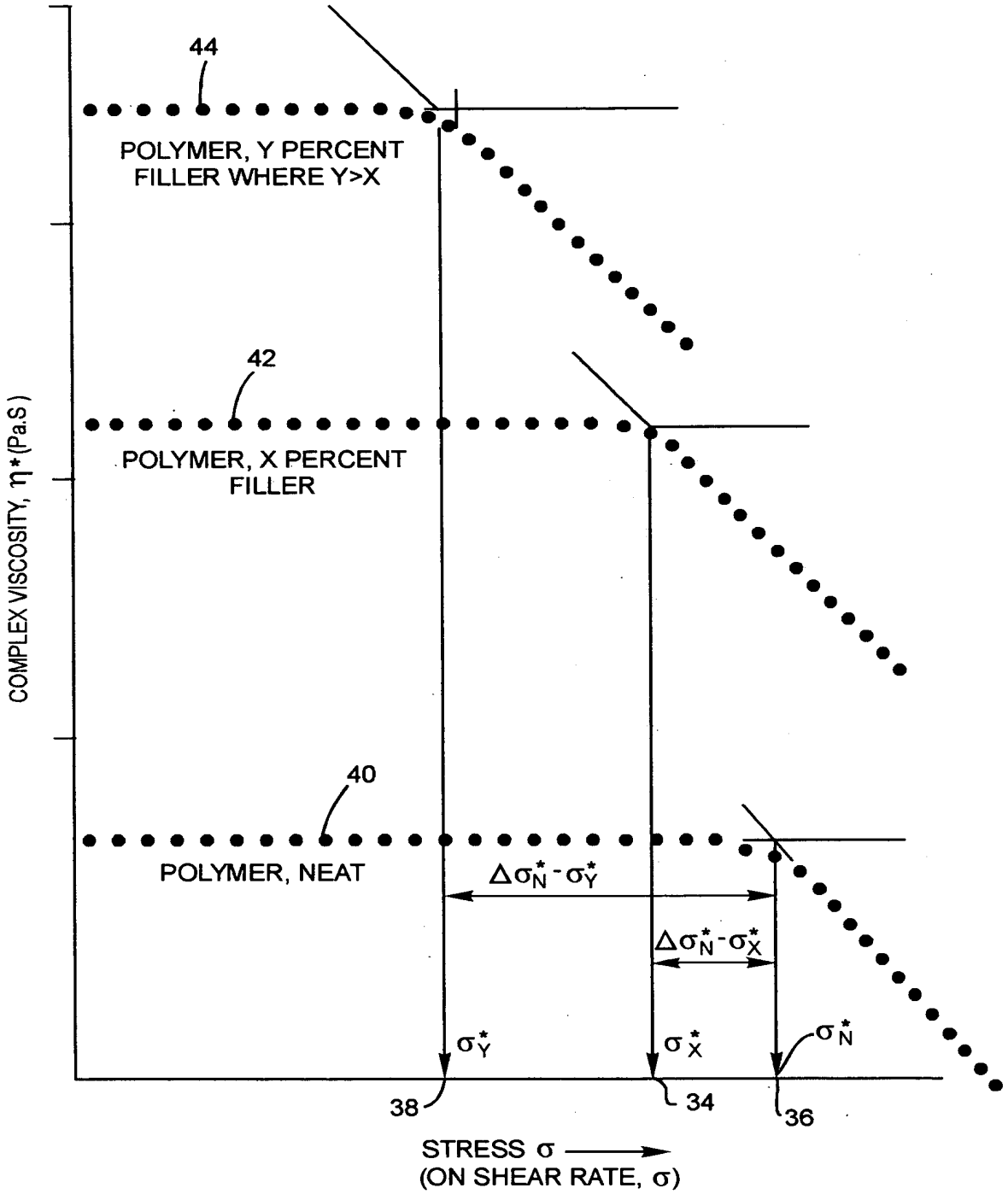

EFFECT OF FILLER, CONCENTRATION ON VISCOSITY AND CRITICAL STRESS VALUE

Fig. 5

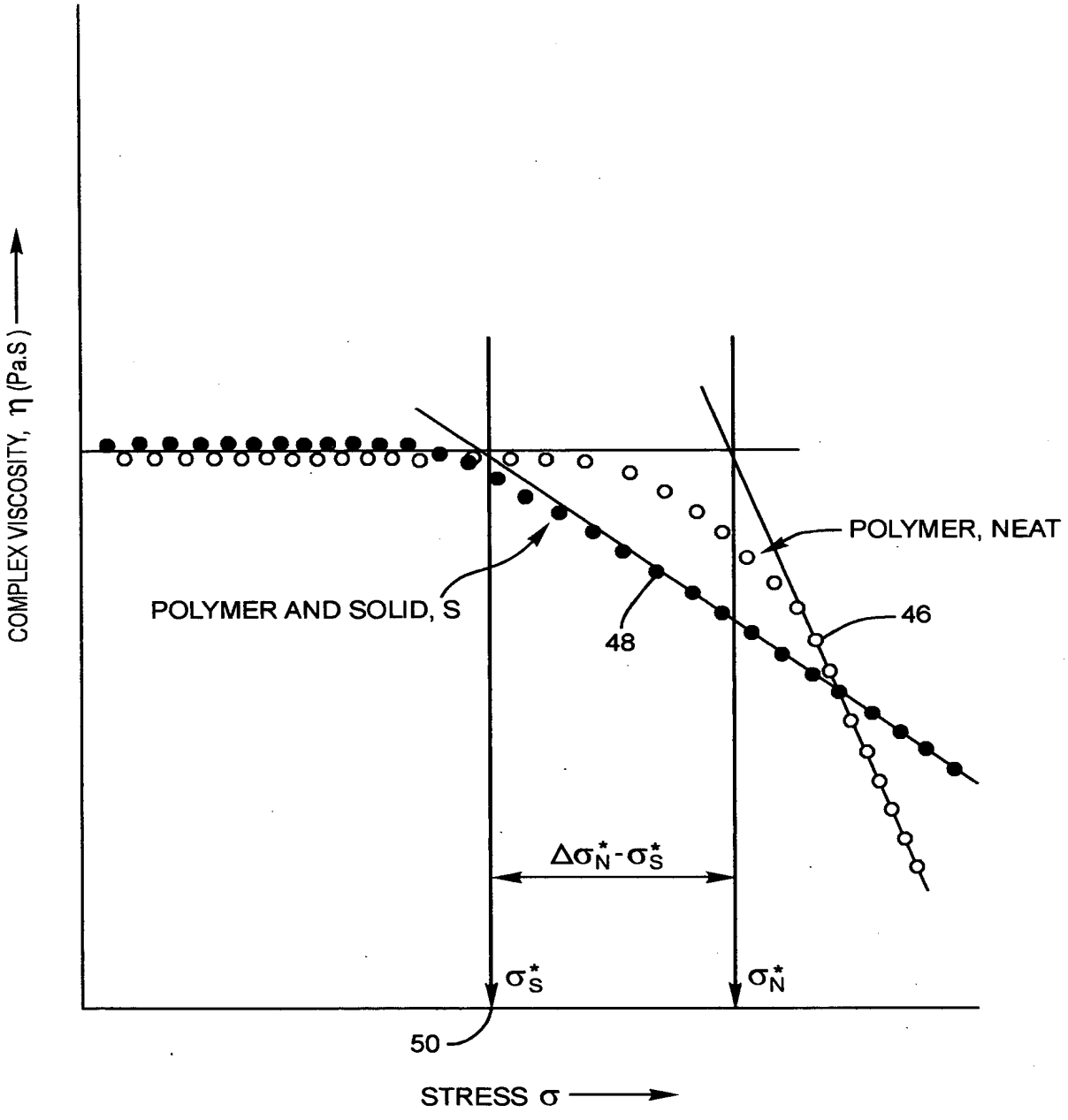

EFFECT ON CRITICAL STRESS VALUE BY ADDING SOLID WITH PREFERRED SIZE RANGE AND CONCENTRATION TO NEAT POLYMER

Fig. 6

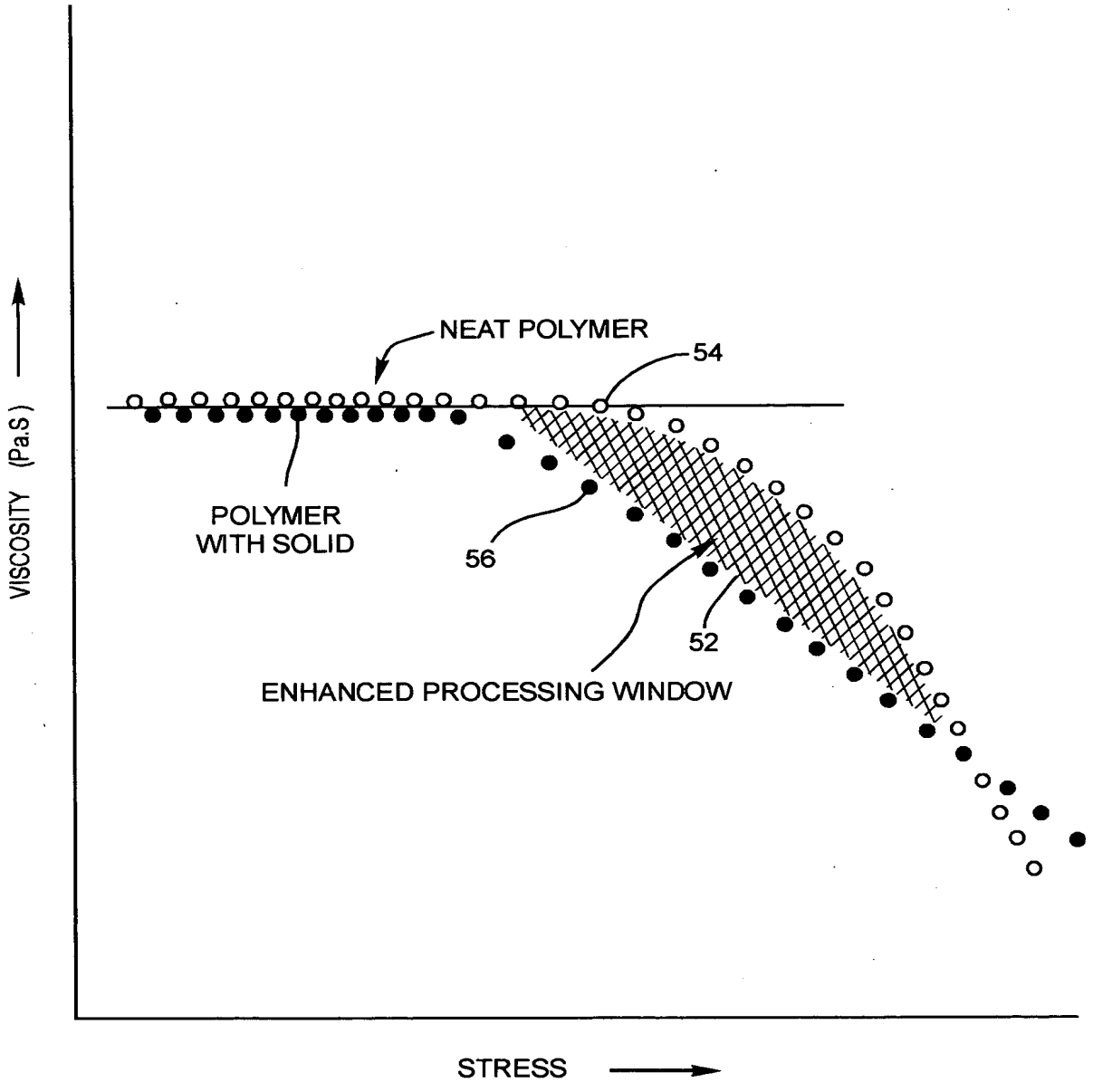

PROCESSING WINDOW FOR UNFILLED POLYMERS

Fig. 7

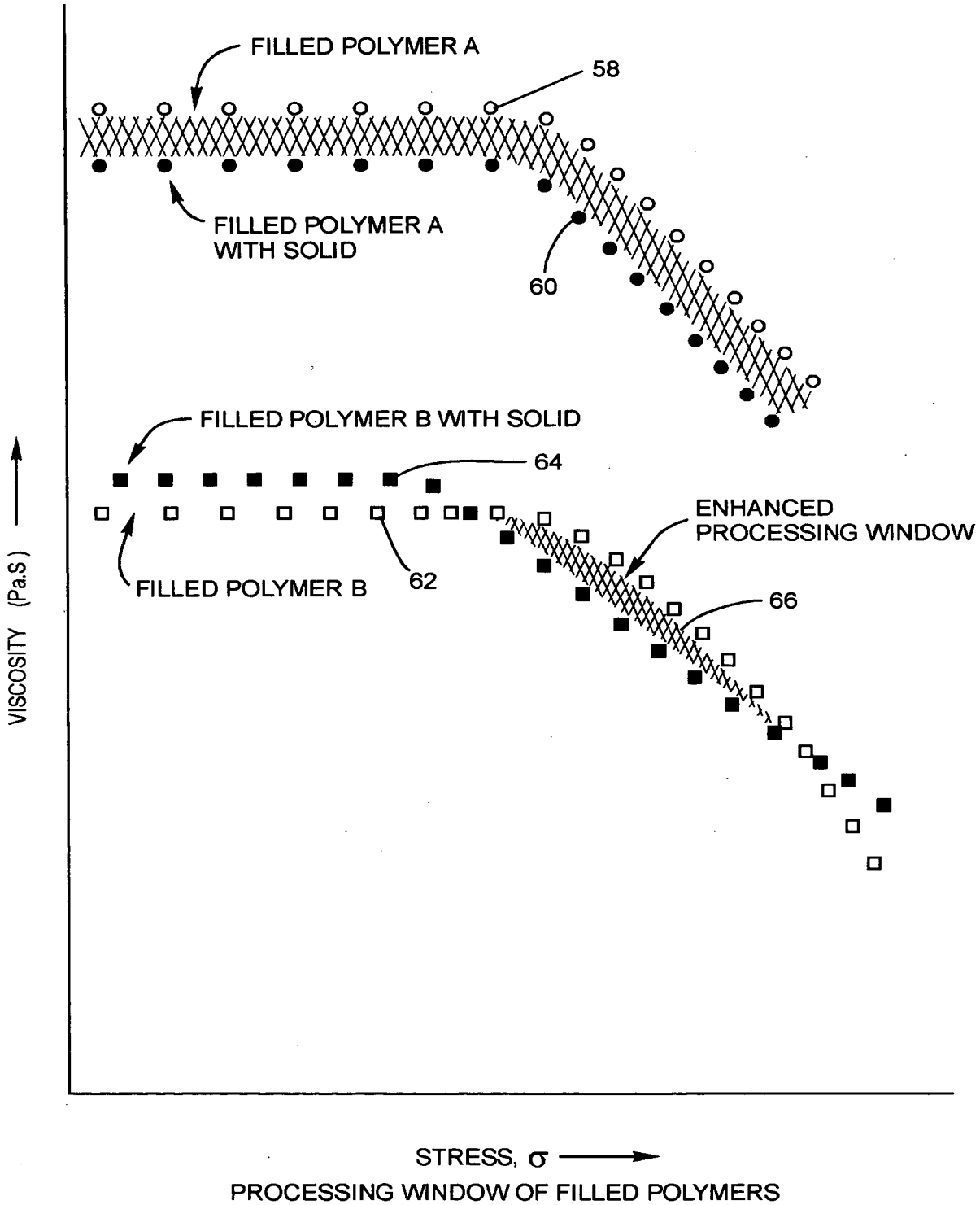

PROCESSING WINDOW OF FILLED POLYMERS

Fig. 8

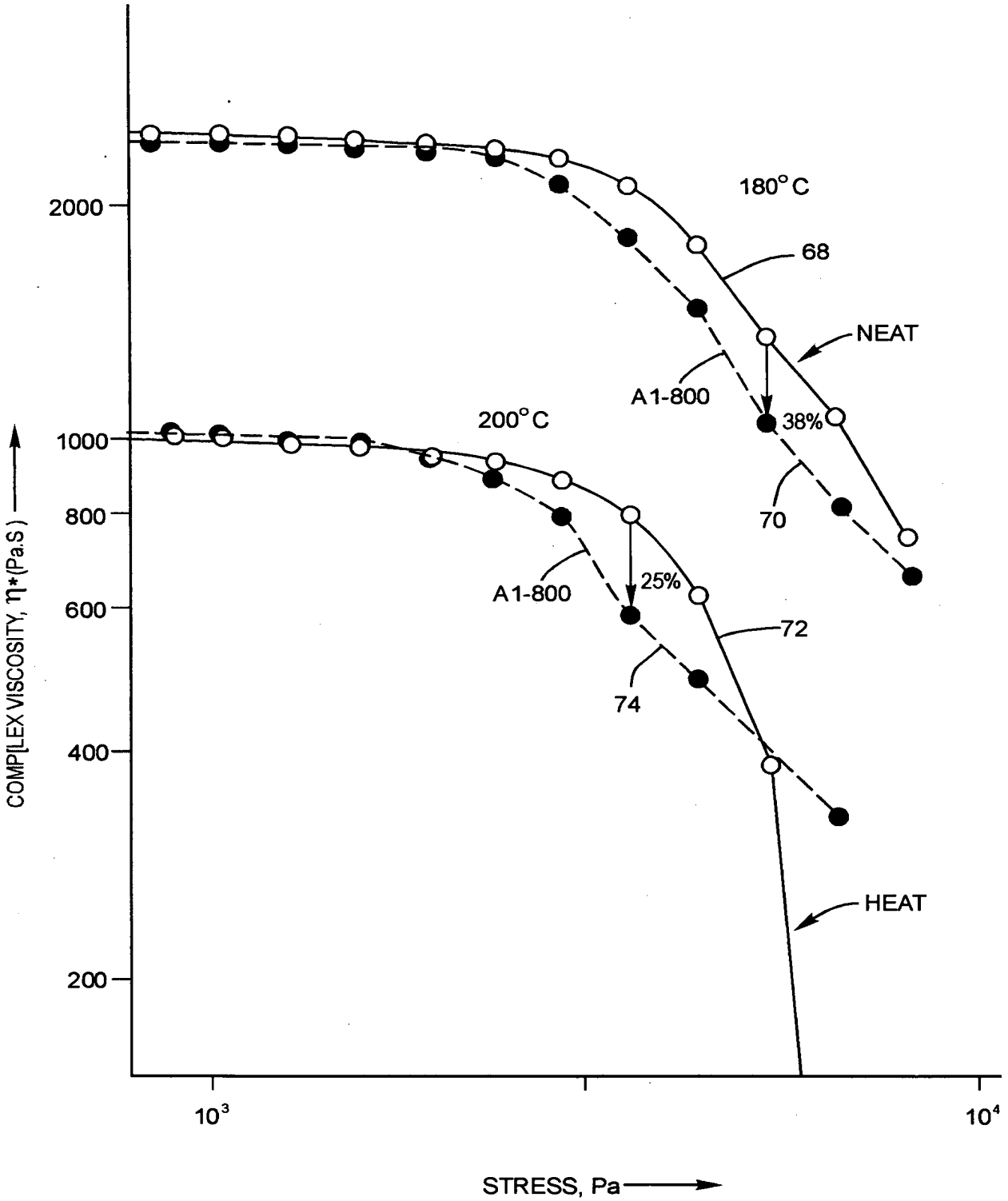

COMPLEX VISCOSITY OF AMORPHONS SOLID A1-800 AND NEAT PP

Fig. 9

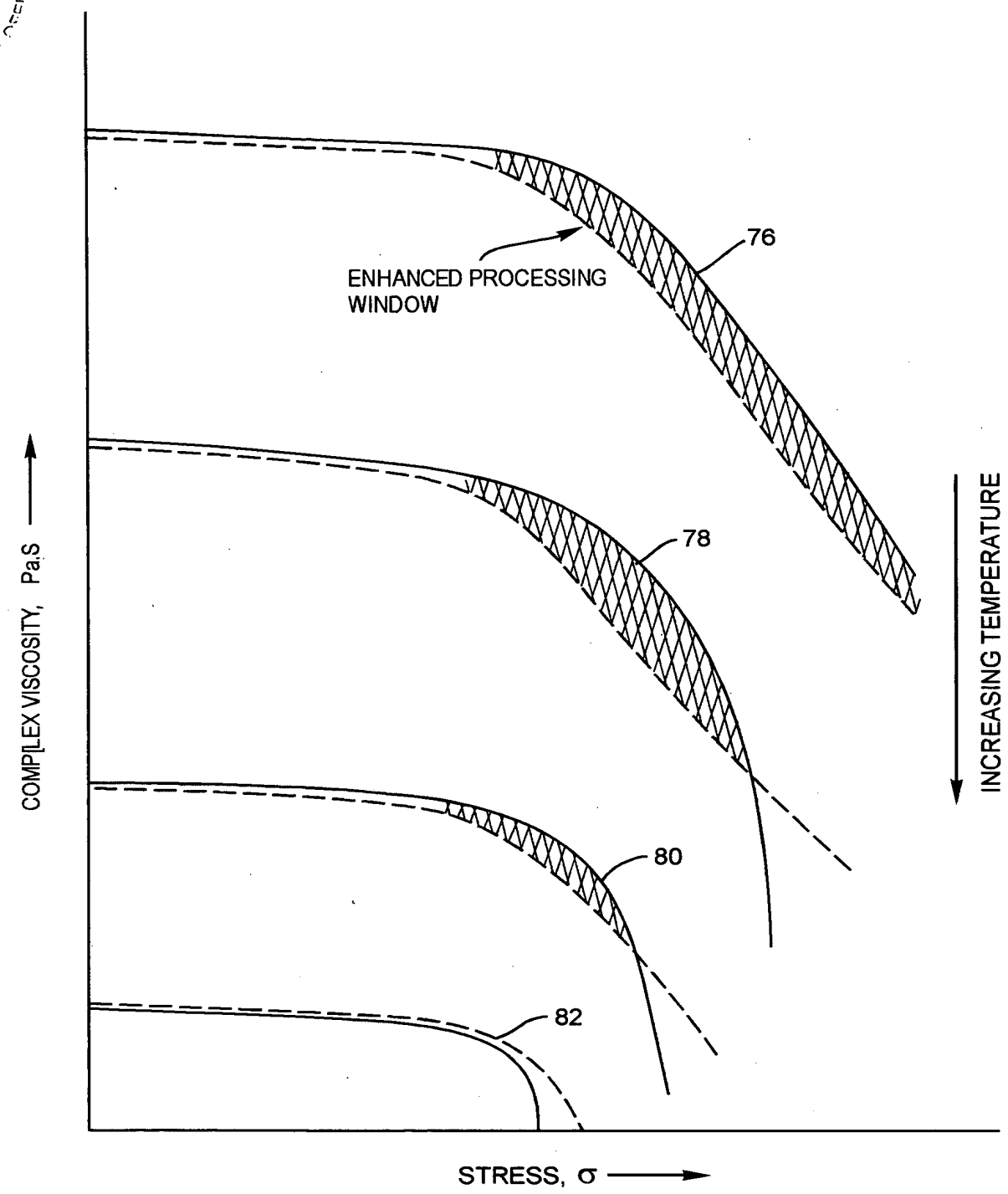

EFFECT OF INCREASING TEMPERATURE ON ENHANCED PROCESSING WINDOW

Fig. 10

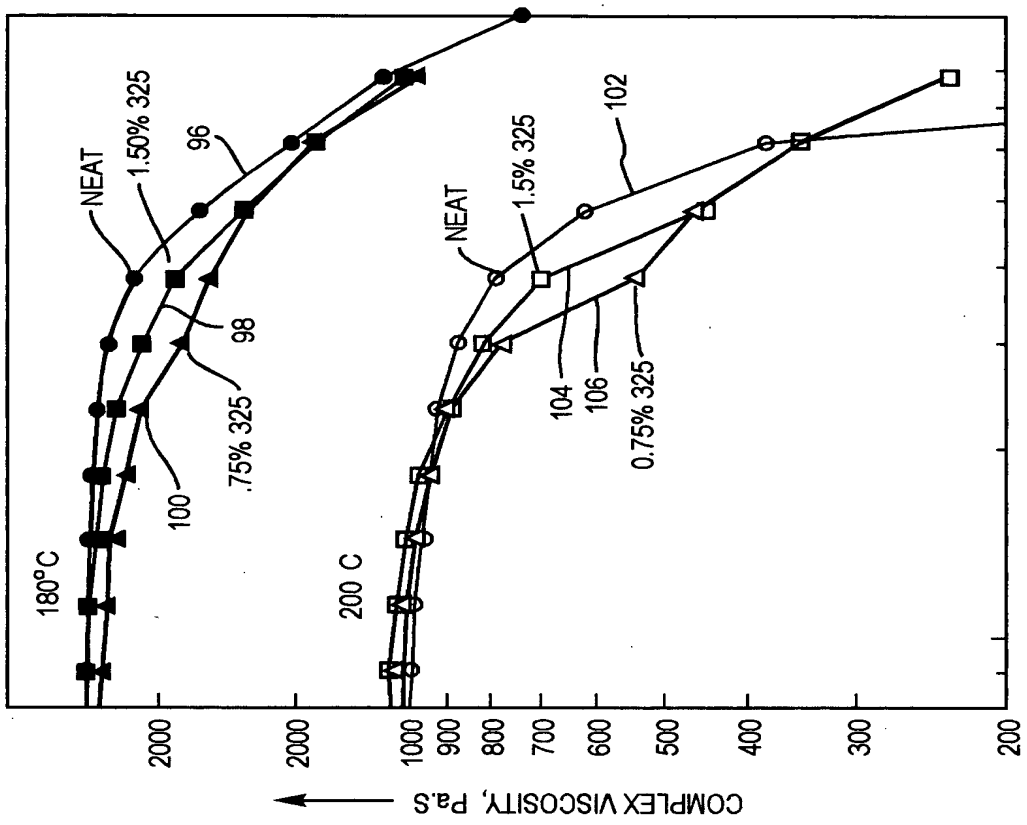

EFFECT OF SOLID CONCENTRATION ON COMPLEX VISCOSITY

Fig. 11B

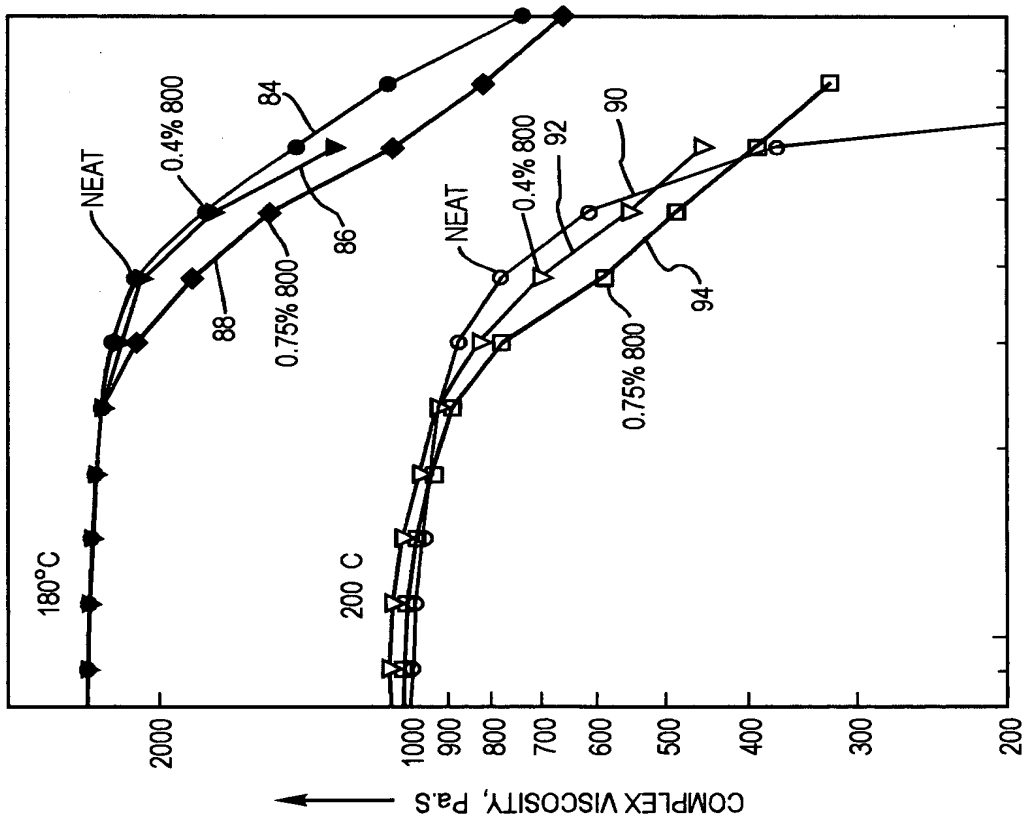

EFFECT OF SOLID CONCENTRATION ON COMPLEX VISCOSITY

Fig. 11A

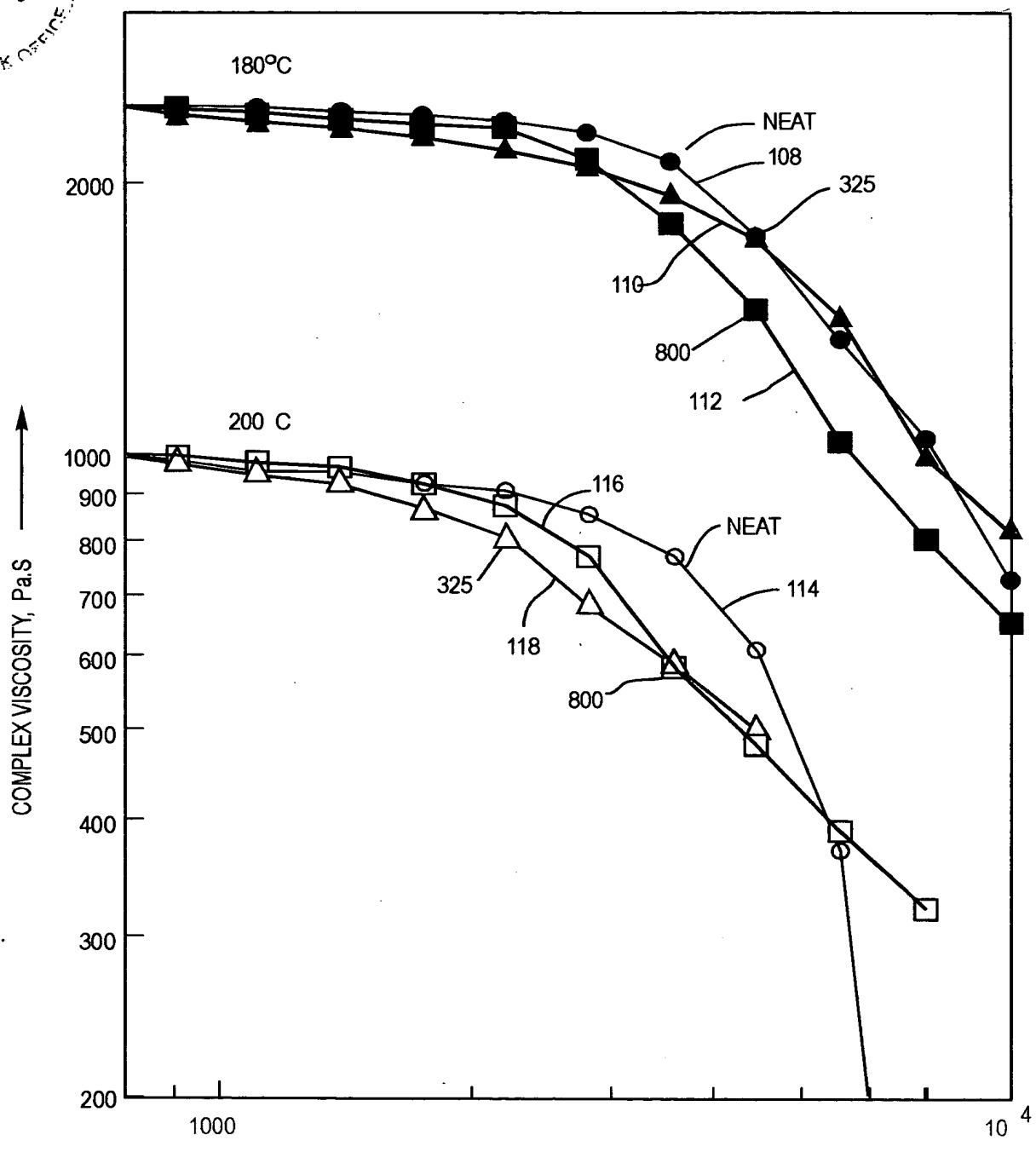

EFFECT OF PARTICLE MESH SIZE ON COMPLEX VISCOSITY

Fig. 12

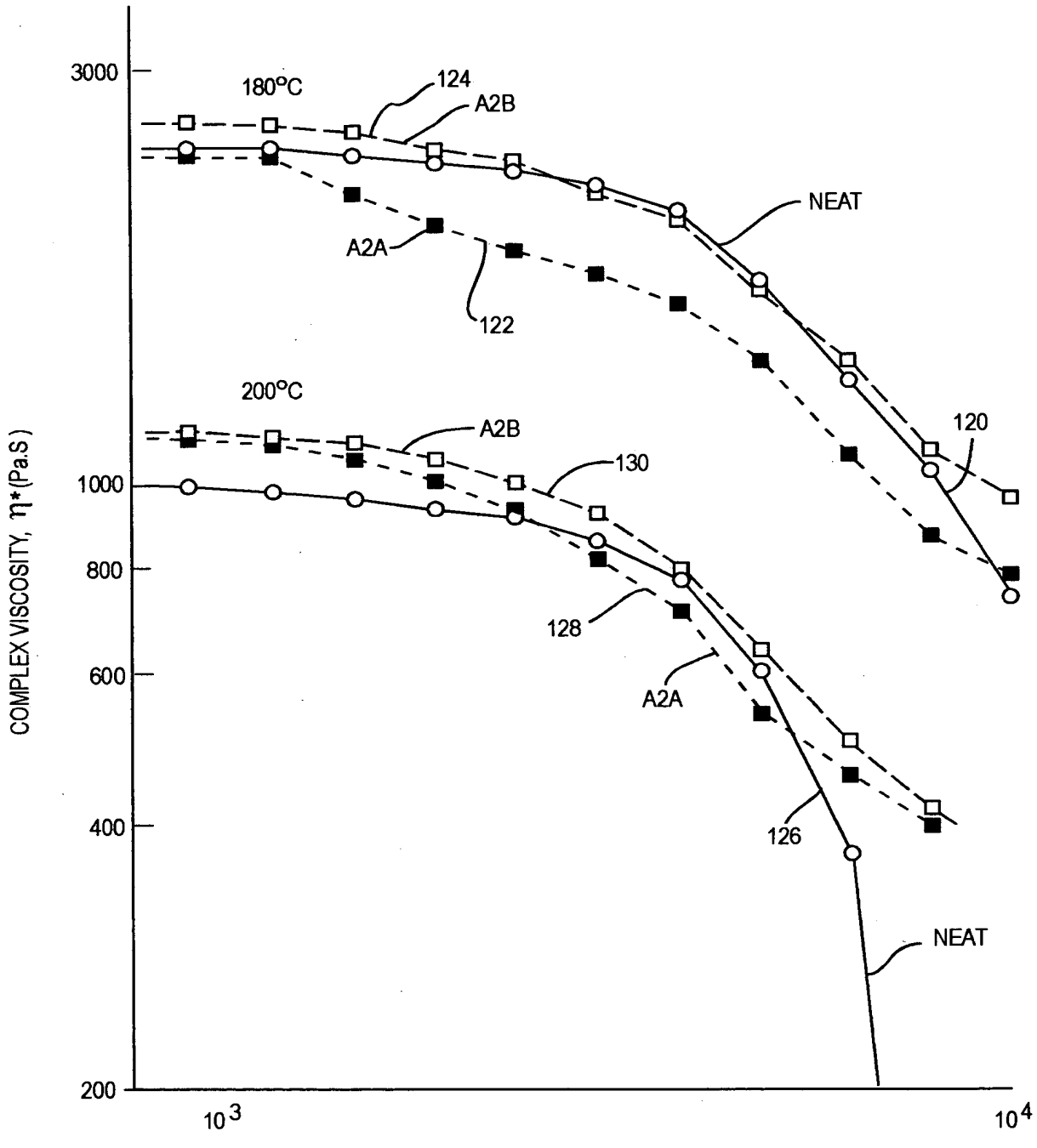

COMPLEX VISCOSITY OF 800-MESH AMORPHOUS SOLID A2 WITH DIFFERENT PARTICLE SHAPES

Fig. 13

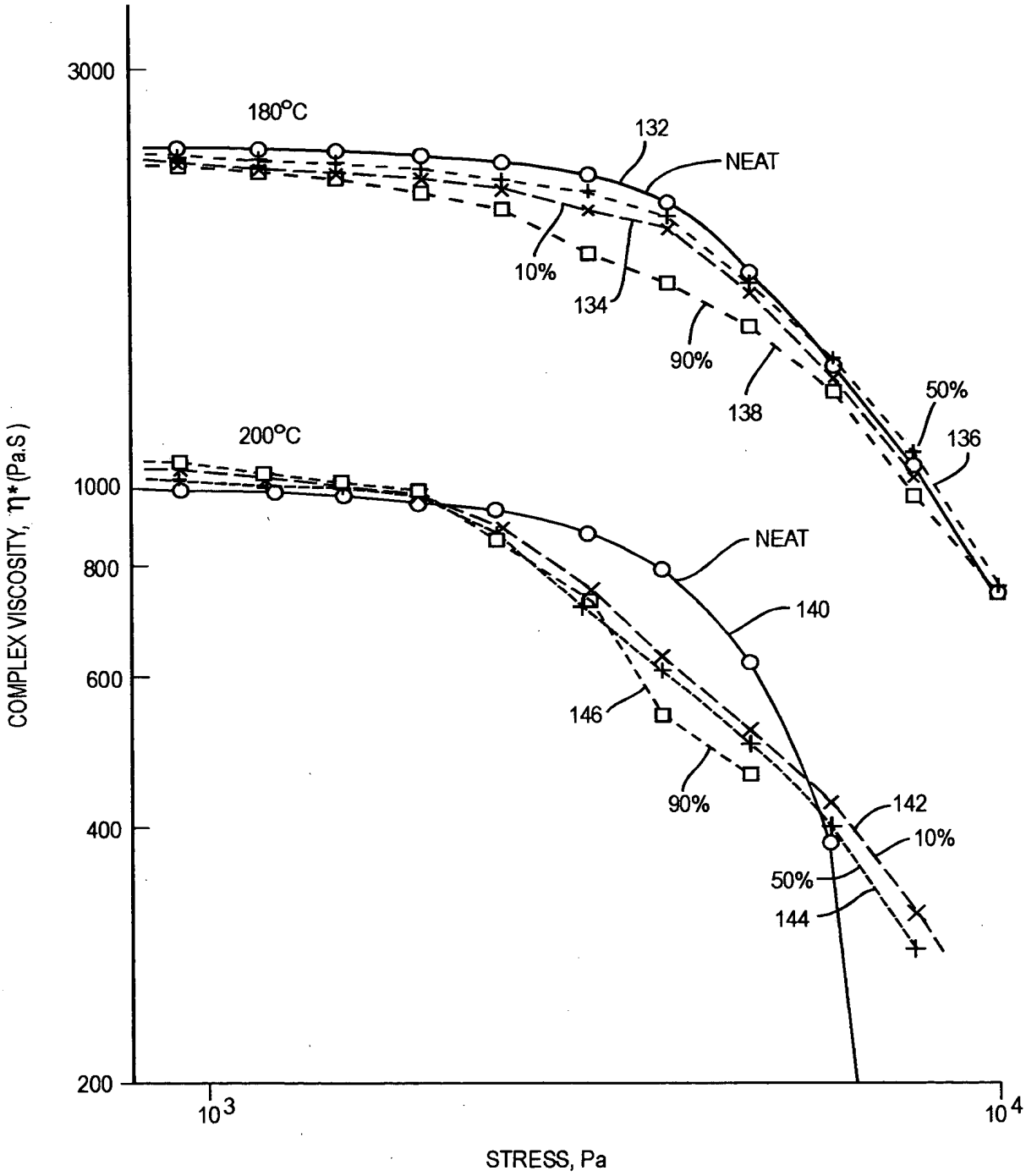

EFFECT OF GLASS CONTENT ON COMPLEX VISICOSITY

Fig. 14

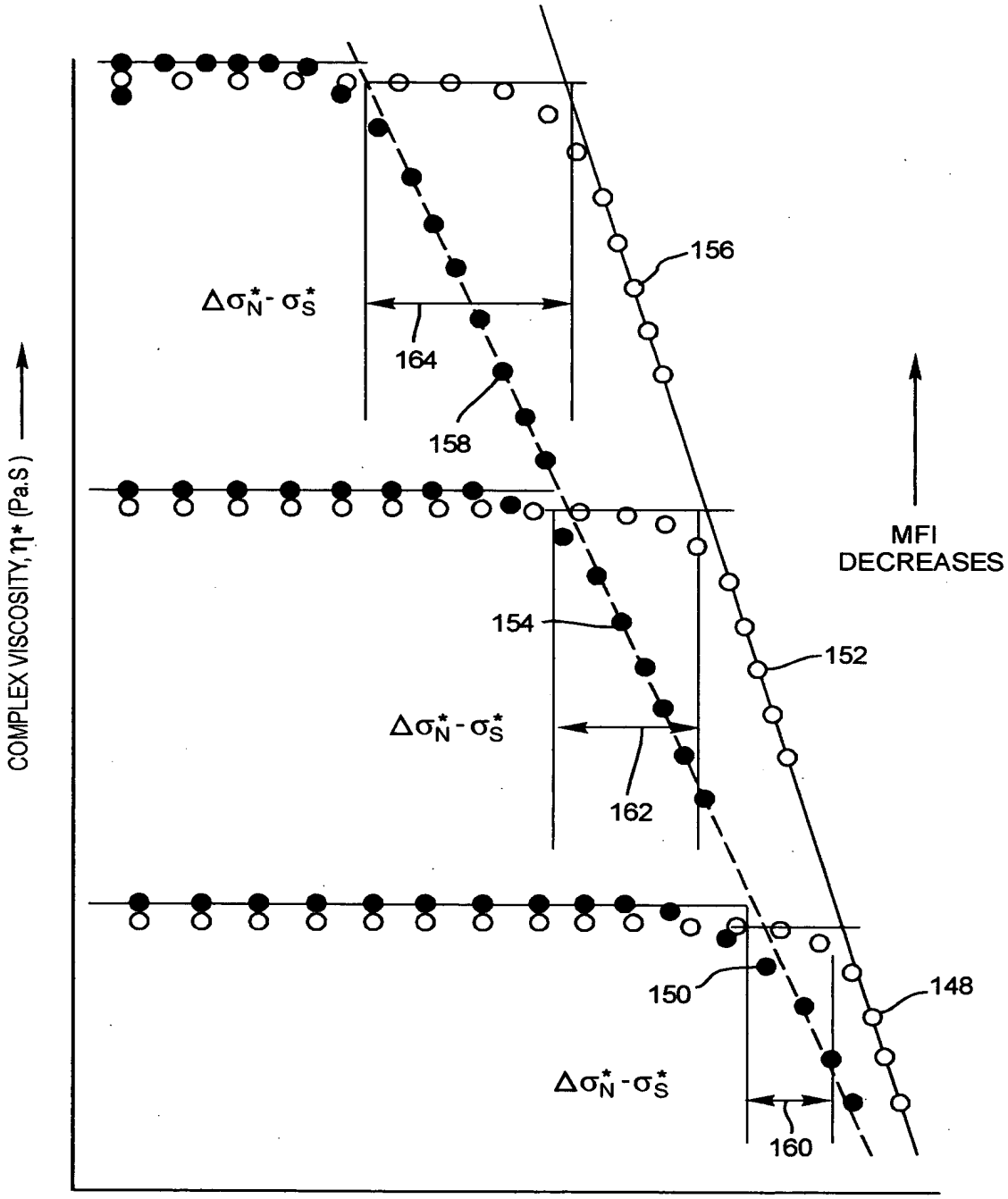

VARIATION IN $\Delta\sigma_N^*$ σ_S^* AS A FUNCTION OF INCREASING MFI FOR A GIVEN POLYMER TYPE

Fig. 15

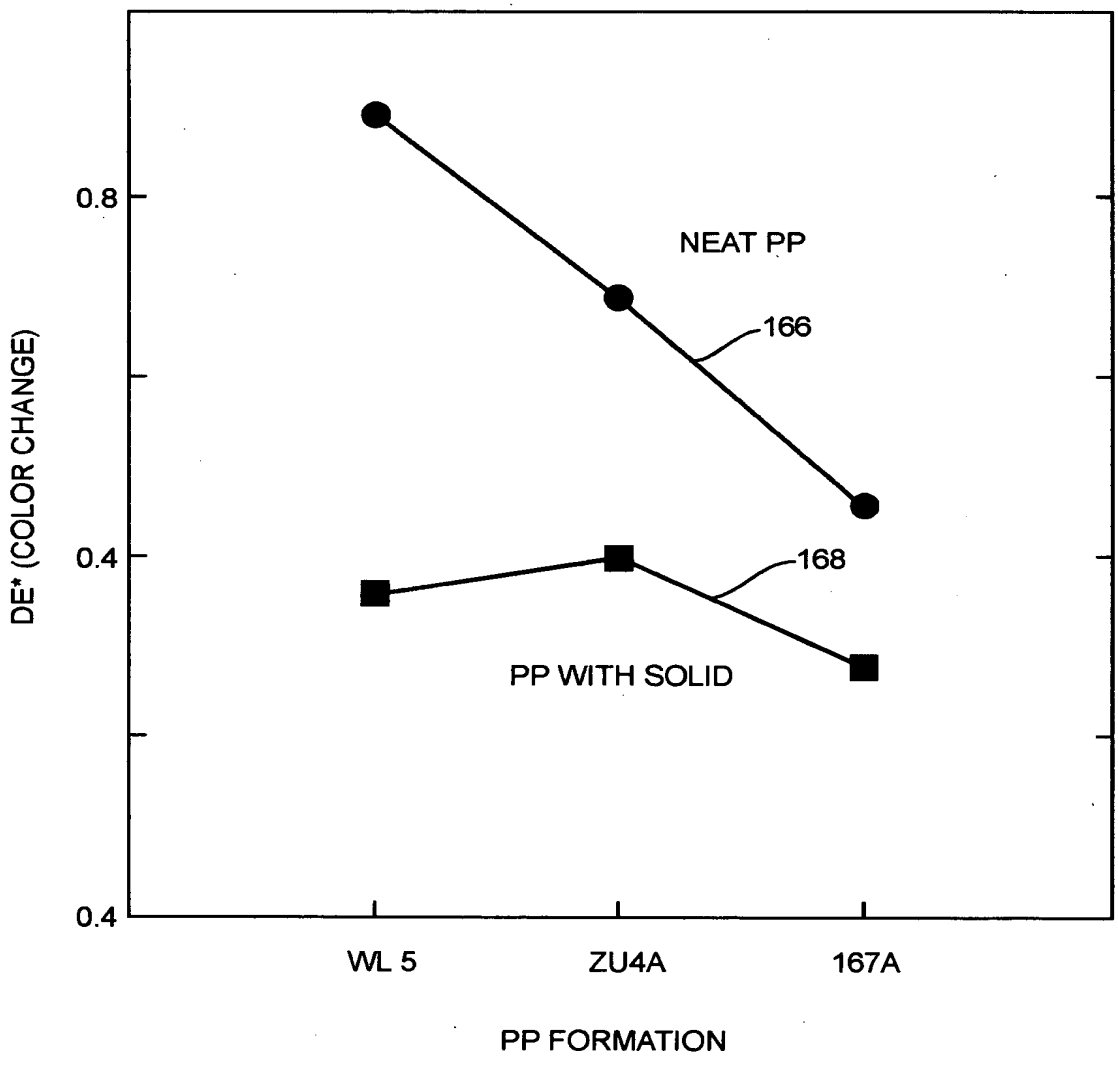

COLOR CHANGE (dE*) IN POLYPROPYLENE AFTER UV LIGHT EXPOSURE

Fig. 16

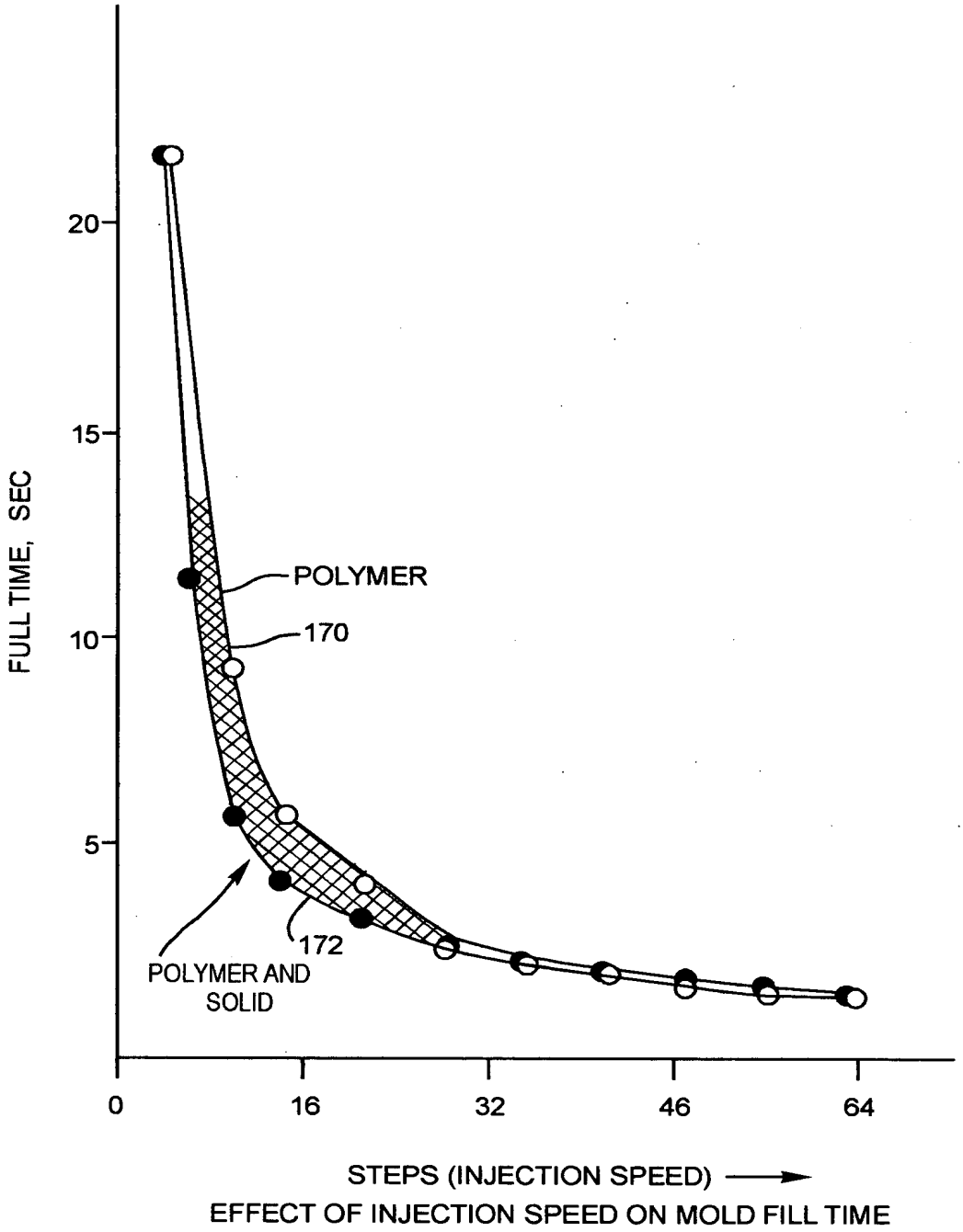

Fig. 17

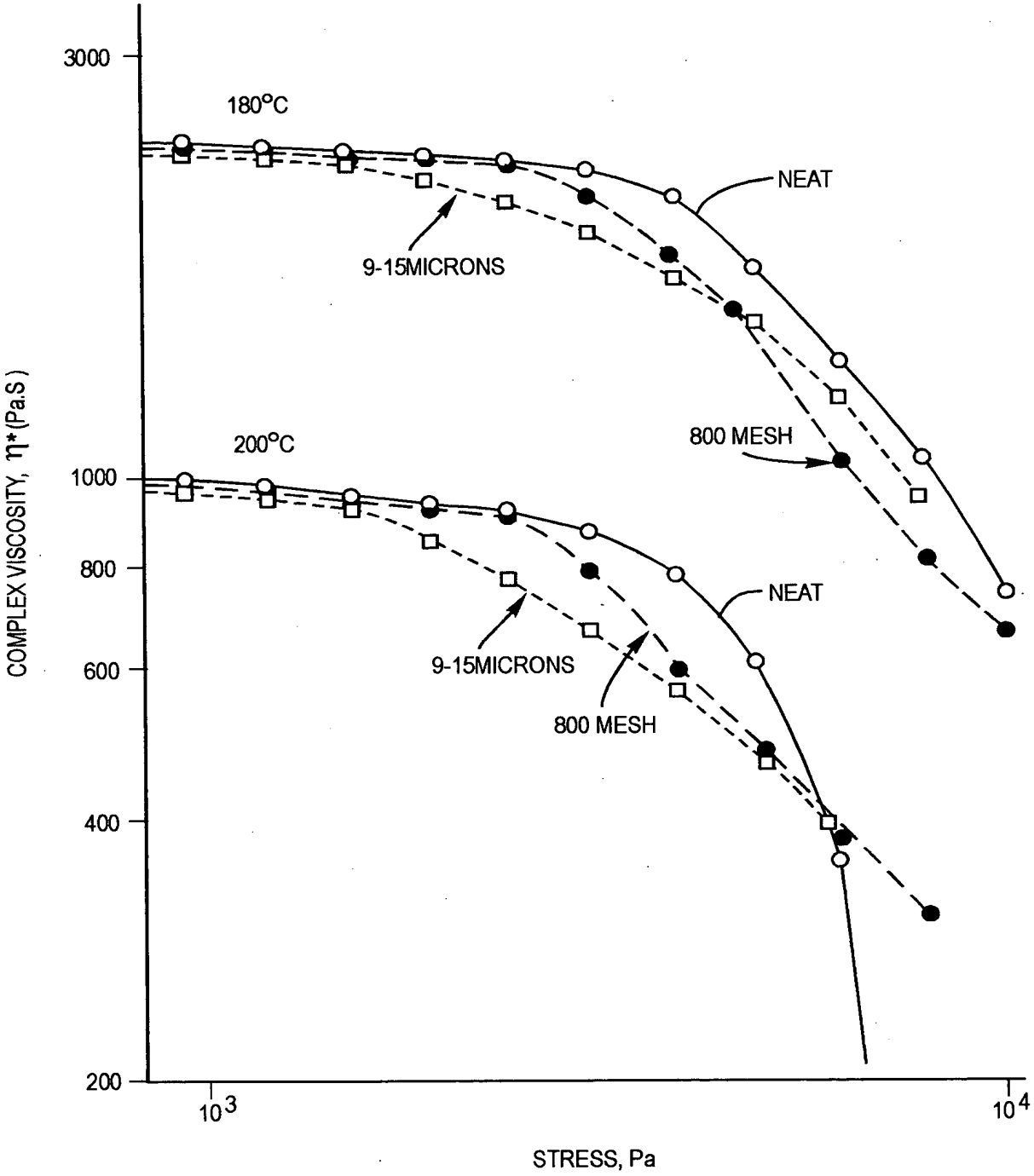

VISCOSITY OF 800-MESH AMORPHOUS SOLID A1 AS COMPARED TO AMORPHOUS SOLID A1 CLASSIFIED TO 9-15 MICRONS

Fig. 18

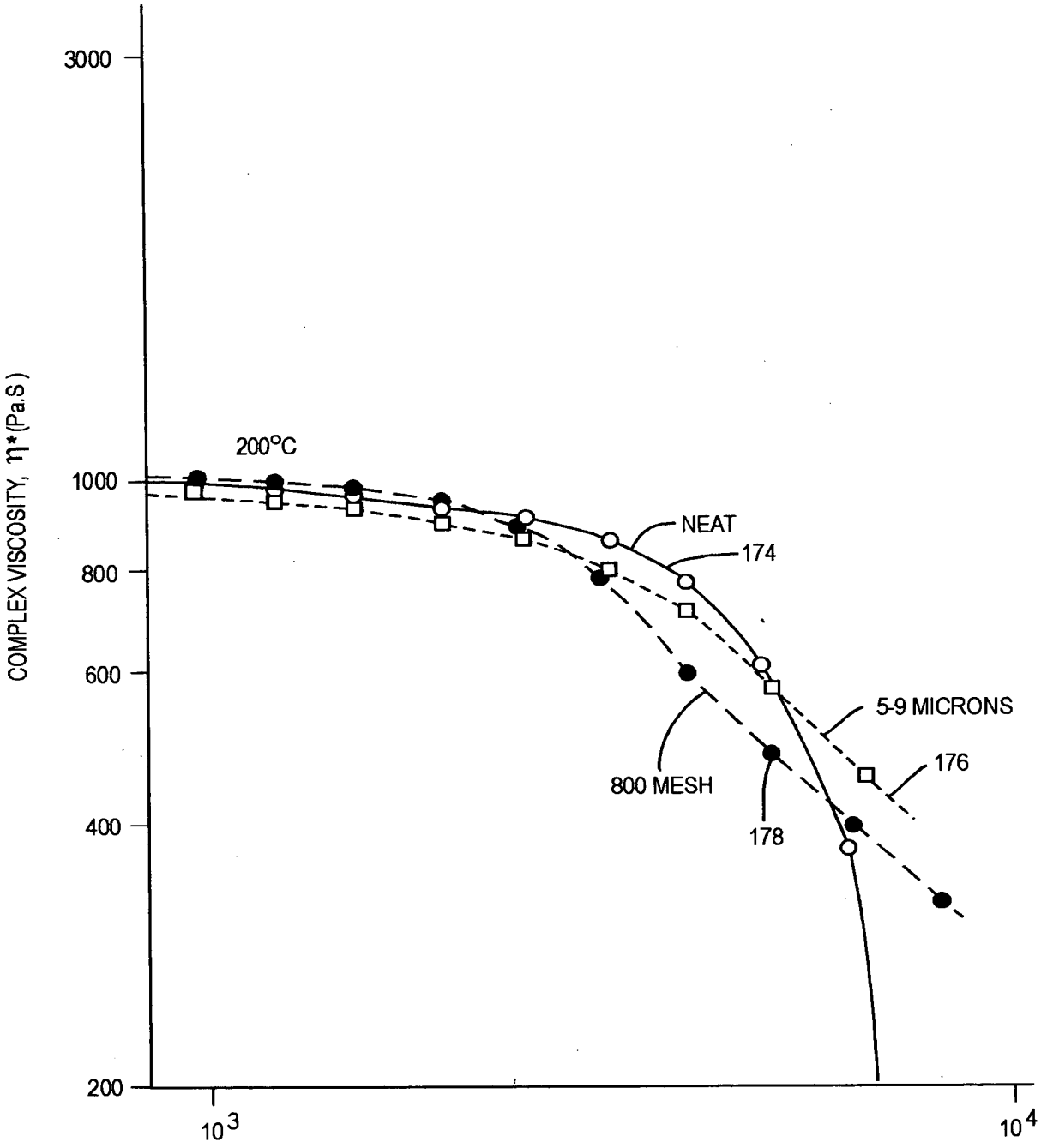

COMPLEX VISCOSITY OF 5-9 MICRON FRACTION OF SOLID A1.

Fig. 19

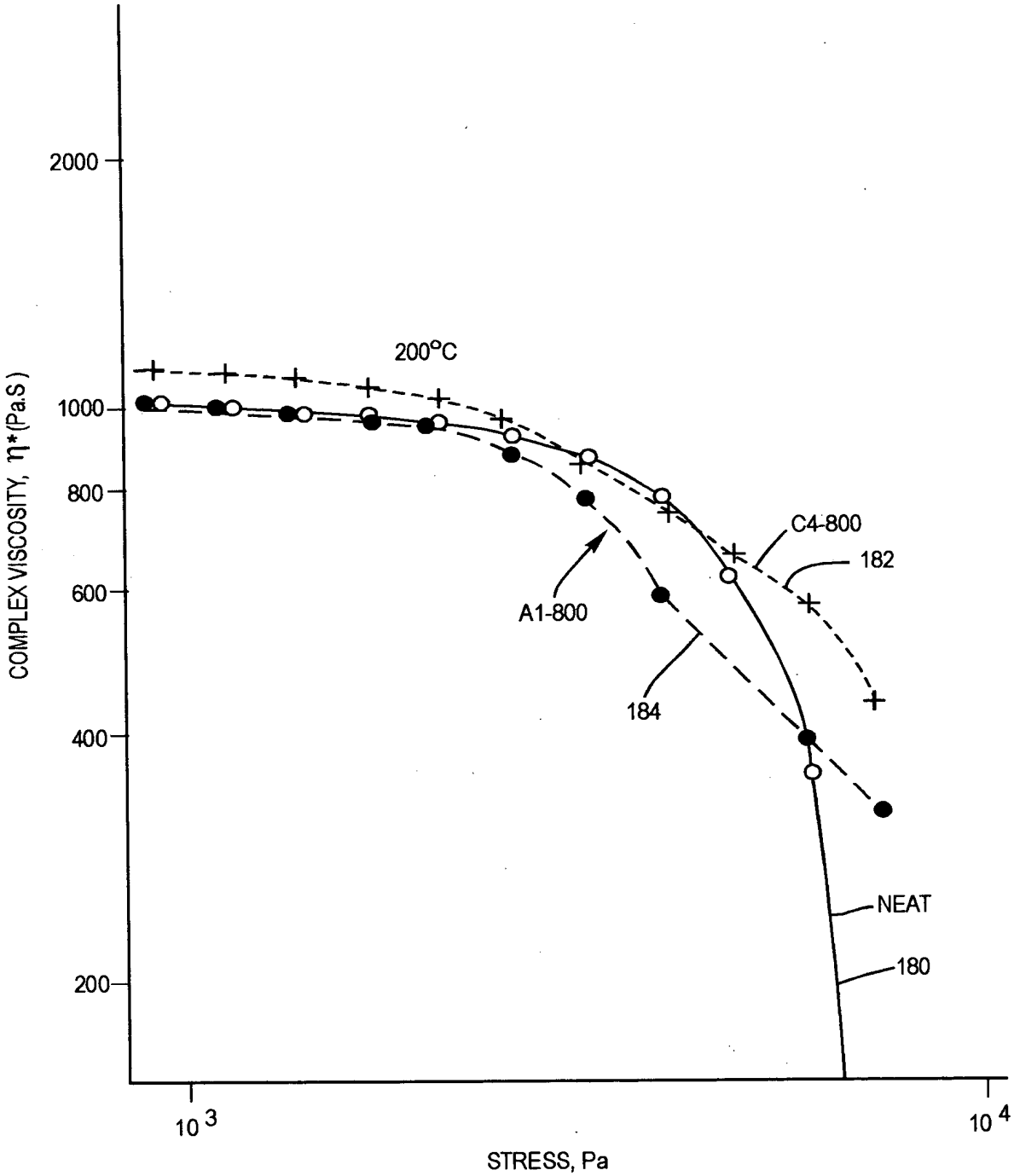

COMPLEX VISCOSITY OF AMORPHOUS MATERIAL, A1-800 MESH, CRYSTALLINE MATERIAL C4-800 MESH AND NEAT PP

Fig. 20

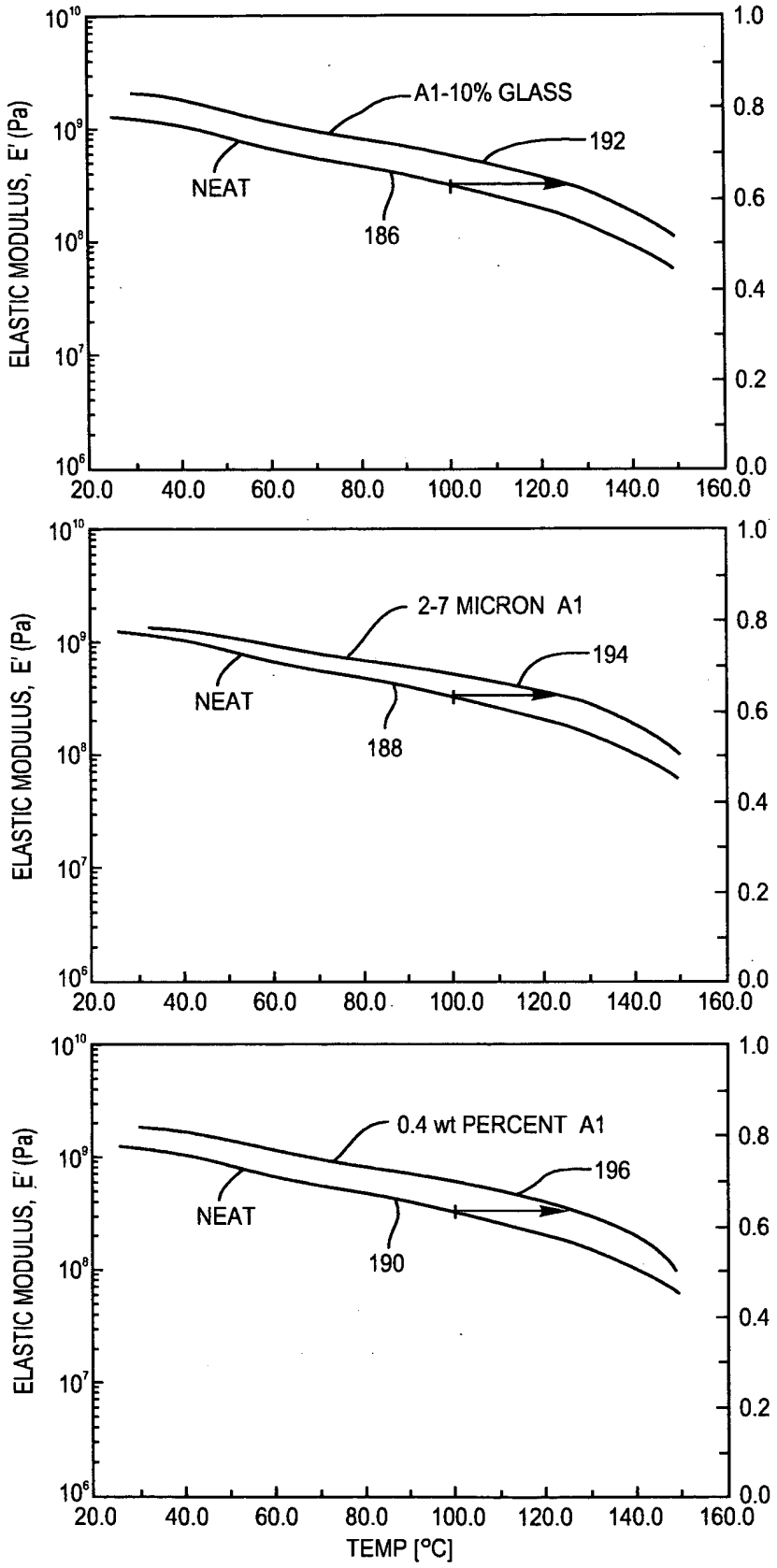

Fig. 21 EFFECT OF PARTICLE CHARACTERISTICS ON DYNAMIC TENSILE ELASTIC MODULUS.